Rotational diffusion of partially wetted colloids at fluid interfaces

Antonio Stocco,[1,2*] Benjamin Chollet,[1] Xiaolu Wang,[1] Christophe Blanc,[1] Maurizio Nobili[1]

[1]Laboratoire Charles Coulomb (L2C), University of Montpellier, CNRS, Montpellier, France

[2]Institut Charles Sadron (ICS), CNRS, 23 rue du Loess, 67034 Strasbourg, France

[*]stocco@unistra.fr, Telephone: +33 (0)388414113, Fax: +33 (0)388414099

Abstract

Hypothesis
Rotational Brownian diffusions of colloidal particles at a fluid interface play important roles in particle self-assembly and in surface microrheology. Recent experiments on translational Brownian motion of spherical particles at the air-water interface show a significant slowing down of the translational diffusion with respect to the hydrodynamic predictions [Boniello et al. Nat. Mat. 14 (2015) 908–11]. For the rotational diffusions of partially wetted colloids, slowing down of the particle dynamics can be also expected.
Experiments
Here, the rotational dynamics of Janus colloids at the air-water interface have been experimentally investigated using optical microscopy. Bright field and fluorescent microscopies have been used to measure the in-plane and out-of-plane particle rotational diffusions exploiting the Janus geometry of the colloids we fabricated.
Findings
Our results show a severe slowing down of the rotational diffusion $D_{r,\perp}$ connected to the contact line motion and wetting-dewetting dynamics occurring on particle regions located at opposite liquid wedges. A slowing down of the particle rotational diffusion about an axis parallel to the interfacial normal $D_{r,\parallel}$ was also observed. Contact line fluctuations due to partial wetting dynamics lead to a rotational line friction that we have modelled in order to describe our results.

Keywords: Rotational diffusion, interfacial diffusion, colloid, air-water interface, viscous drag, line pinning, partial wetting

Graphical Abstract

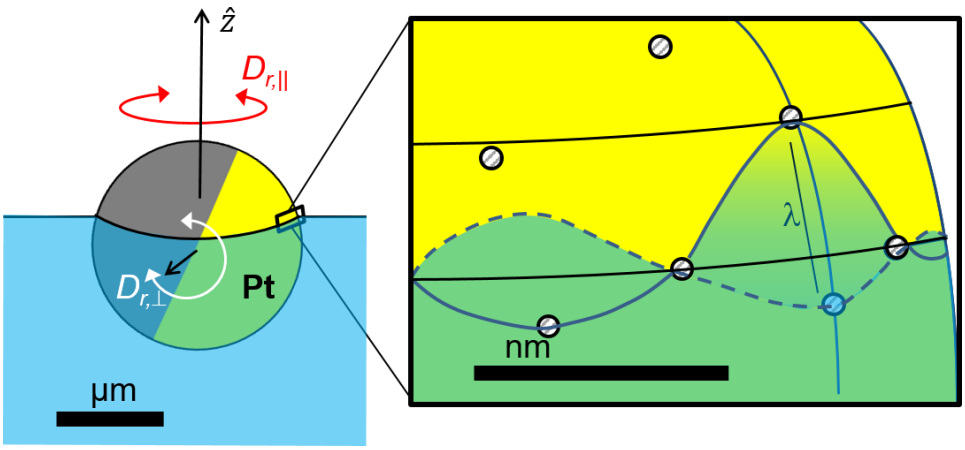

1. Introduction

A solid particle straddling an interface should not be simply seen as a geometrical object partially immersed in a liquid but rather as an intriguing partial wetting configuration. For colloidal microparticles, the fluid interface deformation due to gravity or other external fields is usually weak and the solid particle immersion is set by an equilibrium contact angle in analogy with the partial wetting of a sessile drop on a solid substrate [1]. This configuration, however, should not be considered static since both the colloidal particle and the contact line are subjected to thermal agitation, which results in the particle Brownian motion and in the displacement of contact line back and forth around some equilibrium position [2].

Particles straddling a fluid or a soft interface are encountered in many research fields ranging from Pickering emulsions, self-assembly, flotation, encapsulation, drug delivery, microrheology and microfluidics [3][4][5,6][7][8]. Translational and rotational motions of particles partially immersed at a fluid interface differ strongly from the motions in the bulk [9,10]. The fluid interface indeed interacts with the particle motion via hydrodynamic and capillary interactions. As a consequence, the interfacial hydrodynamics becomes rather complex and models are still lacking even for the rotational motion of simple particles. For example, to the best of our knowledge, only the geometry of an half immersed sphere has been modelled but no general expression of the rotational frictions as a function of the particle immersion has been reported [11]. For the translational motion, hydrodynamic models [11][12–14], which account for viscous dissipations, particle immersion and finite slip lengths, have been developed. Experiments, however, show large deviations from these models [15][16][17]. Recently, the roles of partial wetting dynamics and contact line pinning (neglected in the previous hydrodynamic models) have been pointed out to explain both the slow particle motion across the interface and the particle translational diffusion parallel to the interface [18,19][20][2].

Concerning the rotational motion, for a spherical particle (of radius R) fully immersed in a liquid (with a viscosity η), a unique bulk rotational diffusion coefficient can be defined as $D_{r,b} = k_B T/\zeta_{r,b}$ where $\zeta_{r,b}$ is the bulk viscous rotational friction: $\zeta_{r,b} = 8\pi\eta R^3$ in no slip conditions (and $\zeta_{r,b} = 0$ in full slip conditions). For a spherical particle half immersed in a liquid, the rotational diffusion is not unique and it will differ if the spherical particle rotates about an axis perpendicular or parallel to the interface normal. Hydrodynamics models predict that in the no slip conditions the rotational diffusion coefficients of an half immersed sphere at a gas-liquid interface should be null for $D_{r,\perp}$ ($\zeta_{r,\perp} = \infty$) and twice the bulk value for $D_{r,\parallel}$ ($\zeta_{r,\parallel} = 4\pi\eta R^3$), where $D_{r,\perp}$ and $D_{r,\parallel}$ are the perpendicular and the parallel rotational diffusion, defined considering the interface normal and the particle axis of rotation, respectively [11]. Removal of the contact-line singularity and the effect of a finite slip length b on the particle rotational diffusions (or frictions) were modelled by O'Neill et al.[11]. This model predicts large variations of the rotational diffusions with the particle size. However, for colloidal particles, one finds that for typical values of b and micrometric particle size, predicted $D_{r,\perp}$ (and $D_{r,\parallel}$) differ only slightly from the bulk rotational diffusion $D_{r,b}$ being the interfacial diffusions of the same order of magnitude of the bulk Stokes rotational diffusion.

From an applied point of view, rotational diffusion of a colloid at the fluid interface is a key factor for both the design of particle hybrids and for the control of the active motion of self-propelled particles. In wet routes, particle hybrids are sometimes fabricated exploiting the partial wetting of colloids at a fluid interface[21][22,23]. Adsorption or chemical reactions can be carried only on one partial wetted surface of the particle. Janus or more complex geometry particles have been formed in this way.[18] However to obtain non-symmetric structures, it is crucial that the rotational particle motion is slow enough so that adsorption or chemical reactions occur only on well defined regions of the particle's surface [21]. Still at the single particle level, experiments on the translational and rotational dynamics at fluid interfaces remain very challenging, in particular for particle sizes approaching the nanoscale. Numerical studies have mainly focused on nanoparticles, showing that the continuum description of the free interfacial energy valid for micron-size particles breaks down for truly nanometric particles [24,25].

Rotational Brownian diffusion is also a key parameter that sets the persistence of active motion of self-propelled colloids [26]. Janus spherical silica particles half coated with a thin platinum layer are such particles, self-propelling in presence of hydrogen peroxide[27]. Recently, we have studied their behaviour at the air/water interface. They possess two hydrophilic faces with similar wetting properties and are only partially wetted when trapped at the interface. We have revealed an enhancement of their

two dimensional active motions compared to the bulk [28][29]. In this paper, we report new experimental results on their rotational Brownian motion extending our first observations on the slowing down of the perpendicular and parallel rotational diffusion coefficients, $D_{r,\perp}$ and $D_{r,\parallel}$ [27,29]. A model for the rotational friction is also developed in order to describe our experimental findings.

2. Materials and Methods

2.1 Colloidal particles

Two particle systems have been investigated: (i) fluorescent platinum-melamine resin (Pt-MF) Janus colloids, and (ii) non-fluorescent platinum-silica (Pt-SiO_2) Janus colloids. The first ones were fabricated starting from melamine resin MF particles R = 1.15 ± 0.3 μm (Microparticles GmbH, Germany). Pt-SiO_2 were fabricated starting from silica particles R = 1.06 ± 0.3 μm (Microparticles GmbH, Germany). Particle size measurements by scanning electron microscopy agree with the nominal size and polydispersity provided by the supplier. Both Pt-MF and Pt-SiO_2 Janus colloids were fabricated by physical vapour deposition [30]. Details on the fabrication protocol can be found in [27–29]. Two metal thin layers were deposited on top of colloid monolayers in order to have a stable and homogeneous coating on the particles. On the bare colloids, first 10 nm of titanium and then 20 nm platinum were deposited, see Fig. 1.

2.2 Sample preparation

Dilute colloidal dispersion of Janus particles were sprayed by airbrush deposition on water, which was filled inside a cylindrical container of 10 mm in diameter [2,28]. Area fraction of Janus particles at the interface is very low, << 0.1%. After particle deposition the container was also close in order to reduce water evaporation. All measurements are performed at room temperature (T = 22 °C).

2.3 Particle tracking, image analysis and particle contact angle

Bright field and fluorescence optical microscopies were used for particle tracking and imaging. Up-right and inverted optical microscopes mounted on anti-vibration tables were used. In typical experiments, images of isolated Janus particles were recorded at a rate of 30 frames per second using objective of different magnifications (×32, ×50, ×63 and ×100). The partial coating of platinum on the colloid modifies the light transmission through the particles or the fluorescence of the particle. It is then possible to evaluate Pt region under adequate illumination. Using *IDL* (Interactive Data Language) routines, we treated the raw image sequences and detected the Pt-cap of Janus particles by applying a grayscale threshold. The out-of-plane orientation β of the particle with respect to the interface was evaluated by measuring the absolute value of the visible Pt cap area. The in-plane orientation φ of the particle was instead evaluated by measuring the orientation of the lever arm L connecting the center of the whole particle and the center of the Pt-cap. Tracking of the particle center was done by an *IDL* routine or by using an image correlation-based approach (‘‘Stat Tracker St. Andrews’’) implemented in Labview (National Instruments).

A “Gel trapping” technique was used to measure the particle contact angle [31]. Details on the protocol used can be found in [2]. Briefly, Janus particles were deposited on a gelled water (Phytagel (Sigma-Aldrich) solution, 2% wt. in water) surface at room temperature. Then, the temperature was raised briefly to 90°C in order to let the particles finding the stable contact angles at the air-water interface. Back at room temperature, Janus particles are transfer in a film (Norland Optical Adhesive 81 (NOA81)) which was photopolymerized by UV light. In this way, the polymerized film contained the Janus particles trapped at a complementary position with respect to the air-water interface Scanning Electron Microscopy (SEM) on a FEI Quanta 200 FEG microscope in a tilted configuration was used to evaluate the particle contact angle.

Fig. 1(A) and (B) show SEM pictures corresponding to (gel-trapped) Janus colloidal particles. Pt-MF Janus colloids show contact angles α = 65°±6° and Pt-SiO_2 Janus colloids show α = 64 ± 2° at the air-water interface. It is important to note that bare particles have smooth surfaces with negligible roughness (< 1 nm). Janus colloids instead show surface roughness of about 10 nm, which is comparable with the Pt coated layer thickness. We also noted that the morphology of the coated Pt layer is more

homogenous for silica than MF colloids, probably due a better adhesion of titanium and platinum on silica than MF.

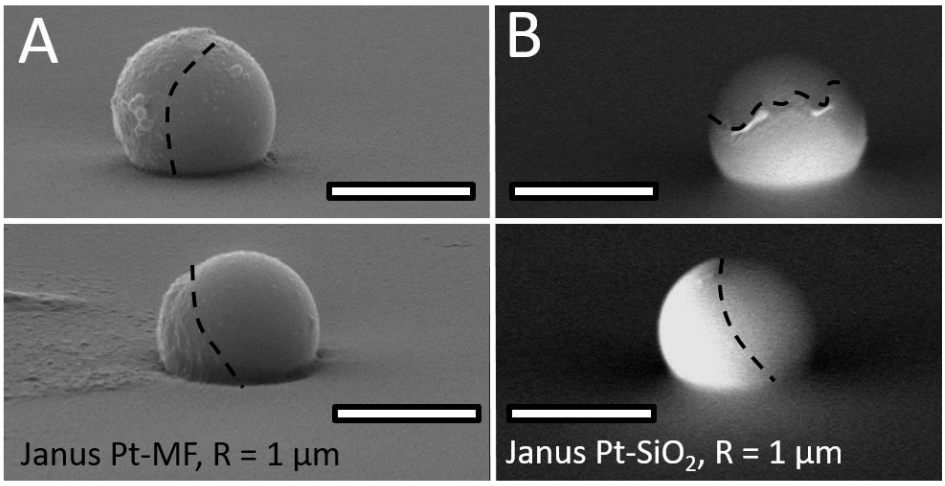

Figure 1 Particles trapped in a polymer layer at the complementary contact angle position with respect to the air-water interface. (A) SEM images of two Pt-MF Janus particles, with a contact angle at the air-water interface of $\alpha \approx 65°$. (B) SEM images of two gel trapped Pt-SiO_2 Janus particles, with a contact angle at the air-water interface of $\alpha \approx 64°$. Dashed lines indicate the Janus boundaries. Scale bars correspond to 2 µm.

3. Results: Rotational diffusion of Janus colloids at the gas-liquid interface

To measure the rotational diffusion of spherical particles, we used Janus particles with two distinguishable faces. If the Janus boundary crosses the fluid interface, particle orientation angles β and φ can be evaluated and rotational diffusions can be measured, see Fig. 2 [27,29].

An example of fluorescent microscopy experiments on Pt-MF Janus colloids at the air-water interface are shown in Fig. 2(A). In these experiments, the Pt cap strongly diminishes the particle fluorescent signal and particle images appear as the crescent moon phases. Hence, the fluorescent region of particle corresponds to the silica area of the colloid, which is not covered by Pt. Subtracting the latter region to the circular area of the entire particle, the Pt cap region can be obtained and its area and orientation fluctuations can be monitored in time, Fig. 2(B) and (C).

Bright field microscopy experiments of Pt-SiO_2 Janus colloids were already described in our previous articles [27,29,32], where the darker side of the particle corresponds to the Pt cap possessing a complex refractive index of $0.48 + 4.87i$ (at 532 nm wavelength, whereas the silica refractive index is $1.46 + 0i$) [27,29,32]. By analysing the images taken during the tracking of the Brownian motion of Pt-SiO_2 Janus colloids at the air-water interface, we were able to evaluate the changes of the absolute area of the platinum cap. We then evaluated the orientation angle β (see Fig. 2(B)) from the visible Pt absolute area, A_{Pt}, knowing that $A_{Pt} = 1/2\pi(1-\cos\beta)R^2$, and calculated the mean square angular displacement $MSAD(\beta)$. In Fig. 3, we plotted $MSAD(\beta)$ as a function of the lag time for three specific datasets corresponding to three different particles for which β varies of ≈40° during 30 s. We fitted the *MSAD* data by:

$$MSAD(\beta) = MSAD_0 + 2D_{r,\perp}\Delta t, \quad (1)$$

where the parameter $MSAD_0$ accounts for the noise introduced by the image treatment. From the fits in Fig. 3, we find that rotational diffusion times $\tau_{r,\perp}=1/D_{r,\perp}$ = 87 s (triangle), 152 s (circle), and 547 s (square) are larger by one order of magnitude or more than the hydrodynamic prediction for particles half immersed in water with finite slip lengths b, $\tau_{r,\perp} = \zeta_{r,\perp}/k_BT$ = 8. 4 s if b = 1 nm ($\tau_{r,\perp}$= 11 s if b = 0.1 nm) [11]. Note that the rotational diffusion time in the bulk is $\tau_{r,b}=1/D_{r,b}$ = 6.3 s, which is of the same order of magnitude of the rotational times calculated with a finite slip length.

In order to discuss these results, we assume the hydrodynamic prediction of $\zeta_{r,\perp}$ for b = 1 nm for half immersed particles [11], and associate an Arrhenius form to the rotational diffusion $D_{r,\perp}$:

$$D_{r,\perp} = \frac{kT}{\zeta_{r,\perp}} \exp\left(-\frac{|\Delta E_\beta|}{k_B T}\right), \qquad (2)$$

where ΔE_β is the activation energy that is required for the out-of-plane change of orientation. Averaging on all *MSAD* data, we found $\Delta E_\beta = 3.6 \pm 0.9\ k_B T$.

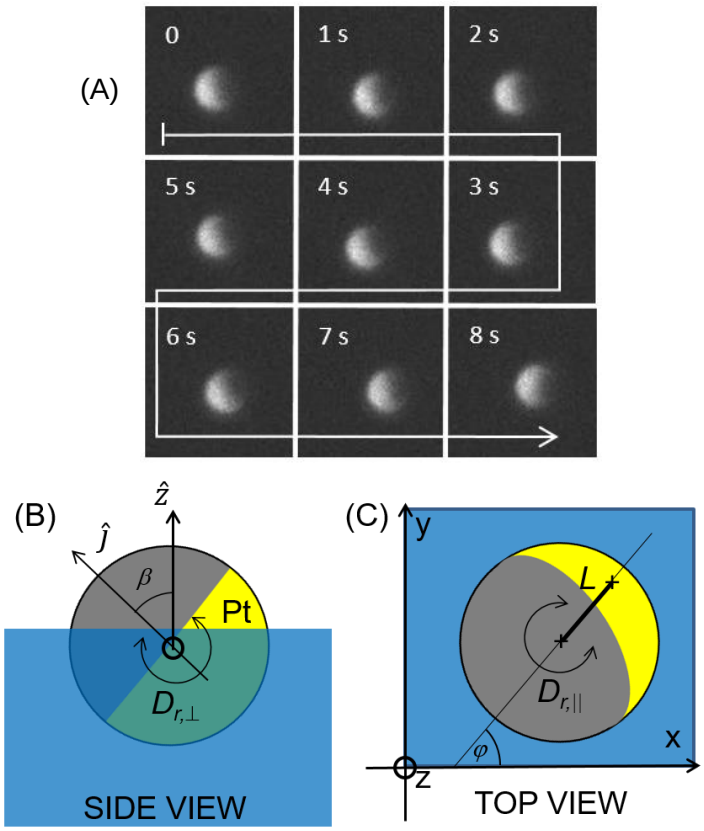

Figure 2 (A) Fluorescent microscopy images of a Pt-MF Janus colloid at the air-water interface taken at different time *t*. The bright region of the particle corresponds to the silica face of the Janus colloid. (B) Side view sketch of a Janus particle at the gas-liquid interface. β is the angle defined by the normal to the interface ($\hat{z}$) and the Janus axis ($\hat{j}$) and $D_{r,\perp}$ is the associated rotational diffusion. (C) Top view sketch of a Janus particle at the gas-liquid interface. L is the lever arm that connects the center of the whole particle and the center of the visible Pt cap. φ is the angle defined by *x*-axis (in the laboratory frame) and the projected direction of L in the *x*-*y* interfacial plane.

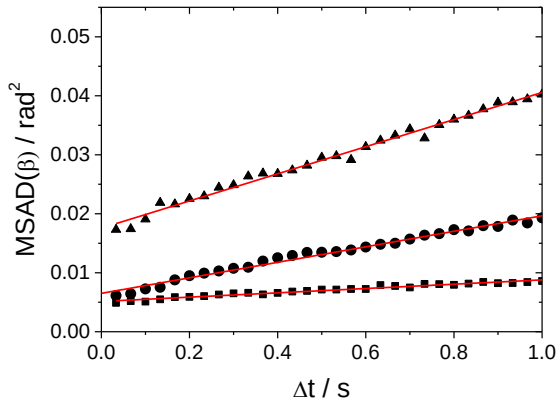

Figure 3 Mean squared angular displacement (*MSAD*) of the out of plane orientation angle β as a function of the lag time for three selected Pt-SiO_2 Janus colloids at the air-water interface. Solid lines represent best fits of $MSAD(\beta) = MSAD_0 + 2D_{r,\perp}\Delta t$.

Now we turn our attention to the in-plane rotational diffusion, see Fig. 2(C). By tracking the motion of fluorescent MF particles partially covered by platinum, we were able to distinguish the fluorescent cap of the colloid from the platinum cap that strongly reduces the particle fluorescence (see Fig. 2(A)). Thus, we calculate the angle φ between the projected Janus axis and the lab frame. φ was evaluated from the orientation of the lever arm L with respect to the laboratory x-y axis in the interfacial plane, see Fig. 2(C). $MSAD(\varphi)$ was calculated for different L/R datasets. In Fig. 4(A), $MSAD(\varphi)$ data show several slopes in different lag time intervals. We fitted the data in the short time limit, for $\Delta t < 0.2$ s, by:

$$MSAD(\varphi) = MSAD_0 + 2D_{r,\parallel}\Delta t. \quad (3)$$

From the fits, we plotted the coefficient $D_{r,\parallel}$ as a function of L/R in Fig. 4(B). $D_{r,\parallel}$ for Pt-MF Janus colloids is surprisingly low. In no-slip conditions, given the particle contact $\alpha \approx 65°$, the diffusion coefficient $D_{r,\parallel} = k_BT/\zeta_{r,\parallel}$ is expected to be in a range between the bulk value of $k_BT/(8\pi\eta R^3)$ and the half immersed particle value of $k_BT/(4\pi\eta R^3)$. Moreover, $D_{r,\parallel}$ should be higher than the latter prediction for positive slip lengths [11]. Except for one measurement, $D_{r,\parallel}$ is however lower than the prediction and it is even lower than the bulk value. In the long lag time limit, most of *MSAD* data show low slopes or even plateaus, which points to confined dynamics probably due to long range capillary interactions, see inset Fig. 4(A) [33–35].

Just for the sake of comparison with $D_{r,\perp}$, $D_{r,\parallel}$ can be also written in an Arrhenius form:

$$D_{r,\parallel} = \frac{kT}{\zeta_{r,\parallel}} \exp\left(-\frac{|\Delta E_\varphi|}{k_BT}\right), \quad (4)$$

where ΔE_φ is the activation energy that is required for a change of orientation φ. For a half immersed particle, $\alpha = 90°$, $\zeta_{r,\parallel} \approx 4\pi\eta R^3$ (if $b = 0.1$ or 1 nm as before) [11]. Given the Janus particle contact angle $\alpha \approx 65°$, we assume here that $\zeta_{r,\parallel} = 1.45\ (8\pi\eta R^3)$ in analogy with the contact angle correction in the model of Fischer et al. for the translational motion [13]. Accounting for all *MSAD* data, we find $\Delta E_\varphi = 1.8 \pm 0.9\ k_BT$. Hence, the slowing down of $D_{r,\parallel}$ is much less severe than the one of $D_{r,\perp}$ as ΔE_φ is smaller than ΔE_β.

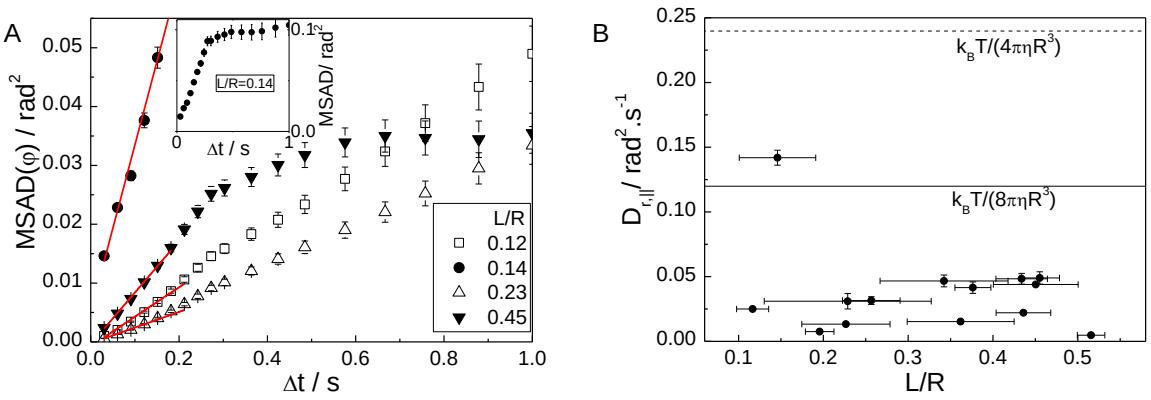

Figure 4 (A) Mean squared angular displacement (*MSAD*) of the in-plane orientation angle φ as a function of the lag time of fluorescent Pt-MF Janus colloids at the air-water interface for different L/R. Solid lines represent best fits of $MSAD(\varphi) = MSAD_0 + 2D_{r,||}\Delta t$ for $\Delta t < 0.2$. (B) Interfacial rotational diffusion $D_{r,||}\Delta t$ as a function of L/R.

4. Discussion: Line friction

As pointed out in Boniello et al. for the slowing down of the translational diffusion of bare particles at the air-water interface, our experimental results cannot be described by current hydrodynamic models that assume a flat and static fluid interface [2]. We suggested that thermally activated deformations at the contact line lead to fluctuating random forces on the particle. We described these fluctuating forces for the translational motion and associated an extra viscous friction on the particle, which leads to a measured translational diffusion slowing down. Here we extend this analysis for the rotational diffusion.

We start summarizing the force calculations for the translational diffusion as reported in Boniello et al. [2]. A fluctuating force F and a torque M acting on the particle can result from an interface deformation due to a contact line displacement, see Fig. 5(A). Considering a short contact line segment l and time t at an angular position Φ_i with respect to an arbitrary axis w in the interface plane, a contact line displacement λ induces a force F and also a torque M on the particle (Fig. 5). Focussing on the force, one can write the component along w by $F_{L,i}(t,l) = F_L^0(t,l)\cos\Phi_i$, where $F_L^0(t,l) = \gamma l(1-\cos\chi)$, where χ is the deformation angle between the horizontal plane and a plane defined by the tangents to the fluid interface at the contact line, see Fig. 5(A) and (B). Several fluctuations may occur along the contact line. Assuming that these fluctuations are not correlated over a finite distance $l=\lambda$, the number n of possible independent fluctuations is:

$$n = 2\pi R\sin\alpha/\lambda \qquad (5)$$

Hence, the total random force is $F_L(t) = \sum_{i=1}^{n} F_{L,i}(t,\lambda)$. One may associate a characteristic time τ_L to the dynamics of $F_L(t)$. For $t > \tau_L$, the mean of this random force should be zero, *i.e.* $< F_L(t) > = 0$. However, the mean squared of $F_L(t)$ is different from zero and equal to:

$$< F_L(t)^2 >= n < F_{L,i}(t,\lambda)^2 >= n < [\gamma\lambda(1-\cos\chi)]^2 > = \frac{1}{2}\, n[\gamma\lambda(1-\cos\chi)]^2 \qquad (6)$$

Hence, this random force due to contact line fluctuations will affect the Brownian motion of the particle. Under some assumptions, one can define a line friction coefficient $\zeta_{t,L}$ associated with the fluctuations of the contact line:

$$\zeta_{t,L} = \frac{1}{2k_BT}\int_{-\infty}^{+\infty} < F_L(0)F_L(t) > \, dt \approx \frac{1}{2k_BT} < F_L(0)^2 > \tau_L \qquad (7)$$

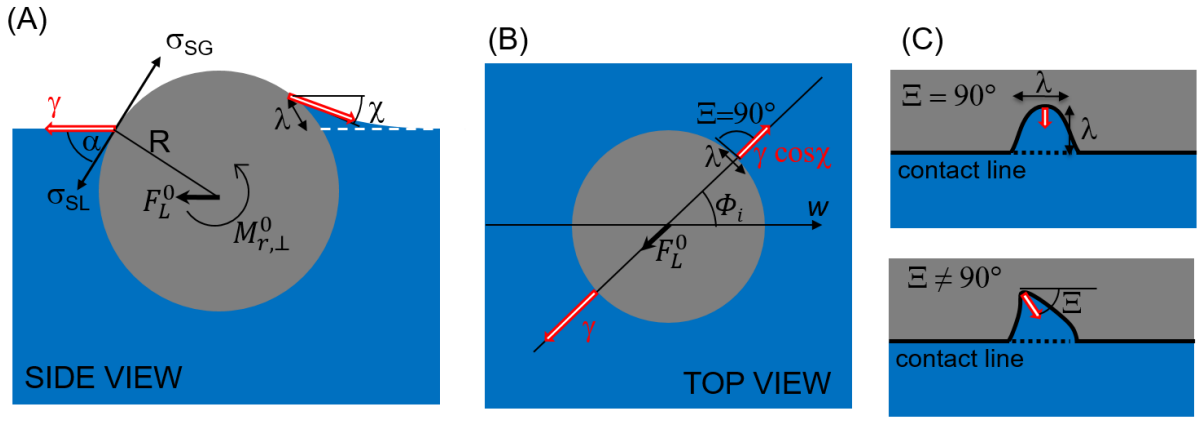

Figure 5 (A) Side view sketch of an interface fluctuation at the contact line. On the left side of the particle, interfacial tensions are in equilibrium and α is the equilibrium contact angle defined by Young's equation. On the right side, an interface fluctuation displaces the contact line on the particle over a distance λ and drives the interfacial tensions out of equilibrium. χ is the angle between the tangent to the fluid interface at the particle and the horizontal. The imbalance between γ and $\gamma\cos\chi$ leads to a force F_L^0 on the particle. (B) Top view of a line deformation, over a segment λ, at the angular position Φ_i. (C) Sketch of a contact line displacement $\lambda\times\lambda$ on the particle surface for $\Xi = 90°$ and $\Xi \neq 90°$.

Note that in Eq. 7 we impose that $< F_L(0)F_L(t) >$ vanishes if $t > \tau_L$. The total friction experienced by the particle is the sum of $\zeta_{t,L}$ and $\zeta_{t,H}$, where $\zeta_{t,H}$ is the hydrodynamic friction, which depends only on the particle immersion and the viscosity [12][13][36].
Eqs. 5, 6 and 7 allow us to write $\zeta_{t,L}$ as:

$$\zeta_{t,L} \approx \frac{1}{4k_BT}\, n[\gamma\lambda(1-\cos\chi)]^2\tau_L = \frac{\pi R\sin\alpha}{2k_BT}\,\lambda[\gamma(1-\cos\chi)]^2\tau_L. \qquad (8)$$

The remaining unknowns in eq. 8 are τ_L and χ. The characteristic time τ_L of the interface fluctuations is given by the molecular kinetic theory of partial wetting [37]:

$$\tau_L \cong \frac{\eta v_m}{k_BT}\exp\frac{E_a}{k_BT} = \frac{\eta v_m}{k_BT}\exp\frac{\lambda^2\gamma(1+\cos\alpha)}{k_BT} \qquad (9)$$

where v_m is the molecular volume of the liquid (v_m = 2.99 10^{-29} m^3 for water) and E_a is the activation energy needed for the line displacement, which can be written as the adhesion energy $E_a = \lambda^2\gamma(1+\cos\alpha)$ [37].

Finally, the deformation angle χ of the interface (Fig. 5(A)) can be found for $n >> 1$ [38].

$$\tan\chi \approx 4\sin\alpha/\pi\,. \qquad (10)$$

Now, we focus our attention on the rotational dynamics. Following the same approach as for the translational friction, the rotational line friction related to $D_{r,\perp}$ (Fig. 2(B)) can be written as [2]:

$$\zeta_{r\perp,L} \approx \frac{1}{2k_BT}\langle M_{L,\perp}(0)^2\rangle\tau_L, \qquad (11)$$

where $M_{L,\perp}$ is the total torque (see Fig. 5(A)) due to contact line fluctuation, $\langle M_{L,\perp}(t)^2\rangle = n\langle M_{L\perp,i}(t)^2\rangle$, and n is given by eq. 5.

A difference between the translational and rotational friction calculations can now be pointed out. If the fluctuation of the contact line corresponds to an advancing line motion (positive vertical displacement, see Fig. 5), corresponding to the wetting of a particle region $\lambda\times\lambda$, the torque on the particle becomes $M_{L\perp}^0(t) = F_1R\cos\alpha - F_2R\sin\alpha$, where $F_1 = \gamma\lambda(1-\cos\chi)$ and $F_2 = \gamma\lambda\sin\chi$. While if the contact line fluctuation leads to a dewetting of a particle region $\lambda\times\lambda$ (negative vertical

displacement), $M^0_{L\perp}(t) = F_1 R\cos\alpha + F_2 R\sin\alpha$. Hence,

$$< M_{L\perp}(t)^2 >= n < M_{L\perp,i}(t)^2 >= \frac{1}{2}\, n[(F_1 R\cos\alpha)^2 + (F_2 R\sin\alpha)^2] \quad (12)$$

The rotational line friction $\zeta_{r\perp,L}$ can be now written as:

$$\zeta_{r\perp,L} \approx \frac{1}{2k_BT}\pi R^3 \sin\alpha \gamma^2 \lambda\, [(1-\cos\chi)^2\cos^2\alpha \quad + (\sin\chi\sin\alpha)^2]\tau_L. \quad (13)$$

where equations 9 and 10 give χ and τ_L.

In Fig. 6, we show that for λ = 0.4 nm at intermediate particle contact angles α, $\zeta_{r\perp,L}$ (equation 13) becomes comparable to the bulk rotational friction, $8\pi\eta R^3$. For $\alpha = 65°$, as for Pt-MF Janus colloids, and λ = 0.6 nm, $\zeta_{r\perp,L}$ is three orders of magnitude higher than the bulk value. Hence λ between 0.4 nm and 0.6 nm could explain our experimental findings showing a severe slowing down of the rotational diffusion $D_{r,\perp}$ (Fig. 2(B)). These values also agree with the value of λ evaluated from the translational friction [2].

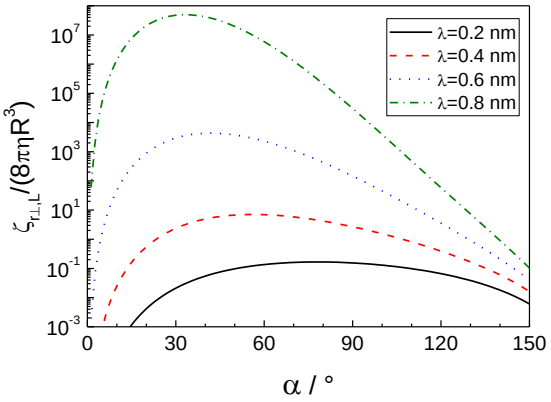

Figure 6 Rotational line friction $\zeta_{r\perp,L}$ divided by the bulk Stokes rotational friction as a function of the particle contact angle for different values of the contact line displacement λ.

Note that the energy ΔE_β in the Arrhenius expression of $D_{r,\perp}$ is related to the adhesion energy in the molecular kinetic theory of partial wetting, which is the energy needed to displace the contact line on the particle surface over a distance λ. Given that the Janus particle surface is not perfectly smooth due to the platinum coating and intrinsic nanometric roughness, this energy is strictly connected to the strength of line pinning [39][2]. An analogy can be also made between the activation energy $E_a = \lambda^2\gamma(1+\cos\alpha)$ in eq. 9 and the activation energy described for the rotation of nanoparticles with defects in molecular dynamics (MD) simulations [40]. In MD simulations for very small nanoparticles with a cylindrical symmetry, the life-time of the nanoparticle metastable orientations depends strongly on the presence of a satellite surface defect, which could lead to life-times from 5 to 10^4 times higher than in absence of the surface defect. Here, surface defects also affect λ that should be considered as an averaged value since the particle is composed of two faces (Pt and silica). Hence, a slowing down of the rotational diffusion $D_{r,\perp}$ can be interpreted in terms of thermal hopping of the contact line as for colloidal particles adsorbing at the oil-water interface [2][18].

Finally, we can discuss the in-plane rotational diffusion $D_{r,\parallel}$ results shown in Fig. 4. A slowing down of $D_{r,\parallel}$ points to the existence of a line friction for the rotational diffusion about an axis parallel to the interfacial normal. However, the model built before for the translational motion and for the rotation about an axis perpendicular to the interfacial normal ($D_{r,\perp}$) assumed that contact line fluctuations lead to forces directed to the vertical axis passing through the center of a perfectly spherical particle (see Fig. 5(B)). Hence in this case, the force acting on the segment λ has no component tangent to the contact line perimeter. Consequently, no fluctuating torque related to $D_{r,\parallel}$ should exist, and a rotational line friction connected to a rotation about an axis parallel to the interfacial normal is not expected. However, a breaking of the particle spherical symmetry could occur for Janus colloids given the non-negligible

thickness and the non-regular shape of the Pt coating. In this case, Janus colloids can be regarded as low aspect ratio ellipsoids for which a rotational line friction was modelled and a slowing down of the rotational diffusion has been experimentally observed [2]. Additionally, one could also consider a generic scenario for which the contact line fluctuations yield both to a radial and an azimuthal force component, F_Φ, able to generate a fluctuating torque parallel to the interface normal, see Fig. 5(C) .

Following the same approach as before, a rotational line friction related to $D_{r,\|}$ can be written as [2]:

$$\zeta_{r\|,L} \approx \frac{1}{2k_BT}\langle M_{L,\|}(0)^2\rangle\tau_L, \tag{14}$$

where $M_{L,\|}$ is the total torque due to contact line fluctuations and $\langle M_{L,\|}(t)^2\rangle = n\langle M_{L\|,i}(t)^2\rangle$, n is given by eq. 5 and:

$$< M_{L,\|}(t)^2 >= n < M_{L\|,i}(t)^2 >= \frac{1}{2}\, n[F_\Phi R\sin\alpha]^2 \tag{15}$$

where $F_\Phi = \gamma\lambda\cos\Xi$, where Ξ is an angle which defines the azimuthal force component F_Φ generating a torque parallel to the interface normal, see Fig. 5(B) and (C). Hence, a rotational friction $\zeta_{r\|,L}$ can be written:

$$\zeta_{r\|,L} = \frac{1}{2k_BT}\pi R^3\sin^3\alpha\gamma^2\lambda\cos^2\Xi\ \tau_L = \frac{\sin^3\alpha}{2}\ \frac{v_m\lambda\gamma^2\cos^2\Xi}{(k_BT)^2}\ \exp\frac{\lambda^2\gamma(1+\cos\alpha)}{k_BT}\pi\eta R^3. \tag{16}$$

Note that for $\Xi = 90°$ (in the ideal case shown in Fig. 5(B)) there is no rotational line friction $\zeta_{r\|,L}$. Since Ξ cannot be calculated or estimated without making several assumptions, in Fig. 7 we plotted the ratio of $\zeta_{r\|,L}$ and the bulk rotational friction as a function of the contact line displacement λ for $\alpha = 65°$ and for three given values of $90° - \Xi = 0.1°$, $1°$ and $10°$. These calculations can be compared with experimental values of $D_{r,\|}$,which are about five times slower than the hydrodynamic prediction. In the range of λ between 0.4 nm and 0.7 nm, the calculated $\zeta_{r,||}$ (eq. 16) agree with the experimental results. However as pointed out before, the value of Ξ cannot be accessed.

Before concluding this section, it is worth noting that particle surface heterogeneity (roughness or defects) would lead not to a single value of contact line displacement but to a range of λ values (and deformation angle Ξ values). For Janus colloids, surface roughness and defects due to the coating fabrication were observed and their distributions seem also non-homogeneous (see Fig. 1). Hence, a distribution of λ (and Ξ) values due to particle surface heterogeneity can be also related to a large distribution of results observed for the rotational diffusions of Janus particles.

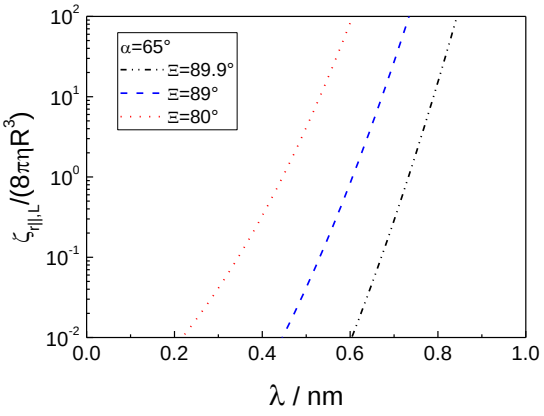

Figure 7 Rotational line friction $\zeta_{r||,L}$ divided by the bulk Stokes rotational friction as a function of the contact line displacement for different values of the angle Ξ (see Fig. 5(B) and (C)).

5. Conclusion

Rotational diffusion of partially immersed particles at a fluid interface has been experimentally investigated focussing on Janus spherical colloids at the air-water interface. The Janus geometry has been exploited to distinguish the two faces of the particle in optical microscopy. Given that two particle's faces have similar wetting properties [27], no strong line pinning on the Janus boundaries has been observed. In this regard, similar results can be expected for non-Janus particles. In agreement with the slowing down of the translational diffusion previously reported for bare spherical and ellipsoidal particles [2], we have observed a slowing down of the rotational diffusion both for the perpendicular and parallel rotations, $D_{r,\perp}$ and $D_{r,\parallel}$ (Fig. 3 and 4). Hydrodynamic models, which assume a flat and calm fluid interface, fail to explain our experiments [11]. In order to describe our results, instead, we have extended a model built for the translational diffusion [2] of bare spherical colloids to the rotational diffusion. In the model, contact line fluctuations and weak line pinning on the surface defects of the particles result in contact line displacement λ, which impacts dramatically the rotational diffusion (Fig. 6 and 7).

The severe slowing down of $D_{r,\perp}$ is in agreement with the experiments reported by Kaz et al. [18] on the slow vertical motion of single colloids breaching a fluid interface. The slowing down in both cases is related to the relative motion of the contact line on the solid particle, and connected to wetting or dewetting processes occurring on the particle surface. The slowing down of $D_{r,\parallel}$ reveals that contact line fluctuations may also lead to force components tangential to the contact line and result in a rotational line friction $\zeta_{r,||}$.

In general, nanoscale roughness and heterogeneity present on the particle's surface have a very strong impact on the interfacial frictions. This result can be rationalised considering that single nanometric defects possess a defect energy of few k_BT, and, in absence of any external field, the diffusion dynamics is driven by thermal agitation (k_BT) only. A large distributions of the rotational frictions were observed, which reflect the dramatic dependence of the rotational frictions to λ variations (Fig. 6 and 7).

The results presented here have clear impacts on the understanding and control of assembly occurring at the fluid interface and in the field of surface microrheology. $D_{r,\perp}$ is in fact a key parameter for the fabrication of Janus particles via adsorption or chemical reactions of partially wetted bare colloids in one fluid phase [8]. $D_{r,\parallel}$ and the associated rotational line friction $\zeta_{r,||}$ plays also a pivotal role in the modelling of passive surface microrheology, because it represents a large contribution to the dissipation measured [7][41].

Perspectives of this work include the role of line pinning strength (weak or strong line pinning) on the contact line frictions, and on how rotational line frictions change in the presence of external fields or persistent velocities as in active microrheology or macrorheology.

Acknowledgements

We acknowledge financial supports from the ANR SURFANICOL ANR-14-CE07-0039-01. We also thank F. Fernandez and the MEA Platform of University of Montpellier for SEM characterizations.

References

[1] A. Stocco, M. Nobili, A comparison between liquid drops and solid particles in partial wetting, Adv. Colloid Interface Sci. 247 (2017) 223–233. doi:10.1016/j.cis.2017.06.014.

[2] G. Boniello, C. Blanc, D. Fedorenko, M. Medfai, N. Ben Mbarek, M. In, M. Gross, A. Stocco, M. Nobili, Brownian diffusion of a partially wetted colloid., Nat. Mater. 14 (2015) 908–11. doi:10.1038/nmat4348.

[3] E. Vignati, R. Piazza, T.P. Lockhart, Pickering Emulsions: Interfacial Tension, Colloidal Layer Morphology, and Trapped-Particle Motion, Langmuir. 19 (2003) 6650–6656. doi:10.1021/la034264l.

[4] A. Scheludko, B. V. Toshev, D.T. Bojadjiev, Attachment of particles to a liquid surface (capillary theory of flotation), J. Chem. Soc. Faraday Trans. 1. 72 (1976) 2815. doi:10.1039/f19767202815.

[5] J. Agudo-Canalejo, R. Lipowsky, Critical particle sizes for the engulfment of nanoparticles by membranes and vesicles with bilayer asymmetry, ACS Nano. 9 (2015) 3704–3720. doi:10.1021/acsnano.5b01285.

[6] J. Agudo-Canalejo, R. Lipowsky, Uniform and Janus-like nanoparticles in contact with vesicles: Energy landscapes and curvature-induced forces, Soft Matter. 13 (2017) 2155–2173. doi:10.1039/C6SM02796B.

[7] P. Dhar, Y. Cao, T.M. Fischer, J.A. Zasadzinski, Active interfacial shear microrheology of aging protein films, Phys. Rev. Lett. 104 (2010) 1–4. doi:10.1103/PhysRevLett.104.016001.

[8] N. Hassan, A. Stocco, A. Abou-Hassan, Droplet Liquid/Liquid Interfaces Generated in a Microfluidic Device for Assembling Janus Inorganic Nanohybrids, J. Phys. Chem. C. 119 (2015) 150505105105007. doi:10.1021/acs.jpcc.5b02527.

[9] H. Brenner, L.G. Leal, A Micromechanical Derivation of Fick ' s Law for Interfacial Diffusion of Surfactant Molecules, J. Colloid Interface Sci. 65 (1978) 191–209.

[10] H. Brenner, L.G. Leal, Conservation and Constitutive Equations for Adsorbed Species Undergoing Surface Diffusion and Convection at a Fluid-Fluid Interface, J. Colloid Interface Sci. 88 (1982).

[11] M.E. O'Neill, K.B. Ranger, H. Brenner, Slip at the surface of a translating–rotating sphere bisected by a free surface bounding a semi-infinite viscous fluid: Removal of the contact-line singularity, Phys. Fluids. 29 (1986) 913. doi:10.1063/1.865686.

[12] K.D. Danov, R. Dimova, B. Pouligny, Viscous drag of a solid sphere straddling a spherical or flat surface, Phys. Fluids. 12 (2000) 2711. doi:10.1063/1.1289692.

[13] T.M. Fischer, P. Dhar, P. Heinig, The viscous drag of spheres and filaments moving in membranes or monolayers, J. Fluid Mech. 558 (2006) 451. doi:10.1017/S002211200600022X.

[14] D. Aaron, S. Hardt, Drag and diffusion coefficients of a spherical particle attached to a fluid interface, J. Fluid Mech. (2015) 1–11. doi:10.1017/jfm.2016.41.

[15] C.-Y. Wu, S. Tarimala, L.L. Dai, Dynamics of charged microparticles at oil-water interfaces., Langmuir. 22 (2006) 2112–6. doi:10.1021/la0525978.

[16] K. Du, J.A. Liddle, A.J. Berglund, Three-dimensional real-time tracking of nanoparticles at an oil-water interface., Langmuir. 28 (2012) 9181–8. doi:10.1021/la300292r.

[17] D. Wang, S. Yordanov, H.M. Paroor, A. Mukhopadhyay, C.Y. Li, H.-J. Butt, K. Koynov, Probing diffusion of single nanoparticles at water-oil interfaces., Small. 7 (2011) 3502–7. doi:10.1002/smll.201101823.

[18] D.M. Kaz, R. Mcgorty, M. Mani, M.P. Brenner, V.N. Manoharan, Physical ageing of the contact line on colloidal particles at liquid interfaces., Nat. Mater. 11 (2012) 138–42. doi:10.1038/nmat3190.

[19] A.M. Rahmani, A. Wang, V.N. Manoharan, C.E. Colosqui, Colloidal particle adsorption at liquid interfaces: Capillary driven dynamics and thermally activated kinetics, Soft Matter. 12 (2016) 6365–6372. doi:10.1039/C6SM00966B.

[20] S. Coertjens, R. De Dier, P. Moldenaers, L. Isa, J. Vermant, Adsorption of Ellipsoidal Particles at Liquid-Liquid Interfaces, Langmuir. 33 (2017) 2689–2697. doi:10.1021/acs.langmuir.6b03534.

[21] K. Fujimoto, K. Nakahama, M. Shidara, H. Kawaguchi, Preparation of Unsymmetrical

Microspheres at the Interfaces, Langmuir. 15 (1999) 4630–4635. doi:10.1021/la990023v.

[22] H. Gu, Z. Yang, J. Gao, C.K. Chang, B. Xu, Heterodimers of nanoparticles: Formation at a liquid-liquid interface and particle-specific surface modification by functional molecules, J. Am. Chem. Soc. 127 (2005) 34–35. doi:10.1021/ja045220h.

[23] B. Liu, W. Wei, X. Qu, Z. Yang, Janus colloids formed by biphasic grafting at a pickering emulsion interface, Angew. Chemie - Int. Ed. 47 (2008) 3973–3975. doi:10.1002/anie.200705103.

[24] D.L. Cheung, S.A.F. Bon, Interaction of Nanoparticles with Ideal Liquid-Liquid Interfaces, Phys. Rev. Lett. 102 (2009) 066103. doi:10.1103/PhysRevLett.102.066103.

[25] D.L. Cheung, S.A.F. Bon, Stability of Janus nanoparticles at fluid interfaces, Soft Matter. 5 (2009) 3969–3976. doi:10.1039/b908462b.

[26] J. Howse, R. Jones, A. Ryan, T. Gough, R. Vafabakhsh, R. Golestanian, Self-Motile Colloidal Particles: From Directed Propulsion to Random Walk, Phys. Rev. Lett. 99 (2007) 048102. doi:10.1103/PhysRevLett.99.048102.

[27] X. Wang, M. In, C. Blanc, P. Malgaretti, M. Nobili, A. Stocco, Wetting and orientation of catalytic Janus colloids at the surface of water, Faraday Discuss. 191 (2016) 305–324. doi:10.1039/C6FD00025H.

[28] X. Wang, M. In, C. Blanc, M. Nobili, A. Stocco, Enhanced active motion of Janus colloids at the water surface., Soft Matter. 11 (2015) 7376–7384. doi:10.1039/c5sm01111f.

[29] X. Wang, M. In, C. Blanc, A. Würger, M. Nobili, A. Stocco, Janus Colloids Actively Rotating on the Surface of Water, Langmuir. 33 (2017) 13766–13773. doi:10.1021/acs.langmuir.7b02353.

[30] J.C. Love, B.D. Gates, D.B. Wolfe, K.E. Paul, G.M. Whitesides, Fabrication and Wetting Properties of Metallic Half-Shells with Submicron Diameters, Nano Lett. 2 (2002) 891–894. doi:10.1021/nl025633l.

[31] V.N. Paunov, Novel Method for Determining the Three-Phase Contact Angle of Colloid Particles Adsorbed at Air - Water and Oil - Water Interfaces, Langmuir. 19 (2003) 7970–7976. doi:10.1021/la0347509.

[32] X. Wang, M. In, C. Blanc, M. Nobili, A. Stocco, Enhanced active motion of Janus colloids at the water surface., Soft Matter. 11 (2015) 7376–7384. doi:10.1039/c5sm01111f.

[33] A. Wittmeier, A. Leeth Holterhoff, J. Johnson, J.G. Gibbs, Rotational Analysis of Spherical, Optically Anisotropic Janus Particles by Dynamic Microscopy, Langmuir. 31 (2015) 10402–10410. doi:10.1021/acs.langmuir.5b02864.

[34] Q. Xu, L. Feng, R. Sha, N.C. Seeman, P.M. Chaikin, Subdiffusion of a Sticky Particle on a Surface, Phys. Rev. Lett. 106 (2011) 228102. doi:10.1103/PhysRevLett.106.228102.

[35] P. Castro-Villarreal, A. Villada-Balbuena, J.M. Méndez-Alcaraz, R. Castañeda-Priego, S. Estrada-Jiménez, A Brownian dynamics algorithm for colloids in curved manifolds, J. Chem. Phys. 140 (2014) 214115. doi:10.1063/1.4881060.

[36] C. Pozrikidis, Particle motion near and inside an interface, J. Fluid Mech. 575 (2007) 333. doi:10.1017/S0022112006004046.

[37] T.D. Blake, The physics of moving wetting lines., J. Colloid Interface Sci. 299 (2006) 1–13. doi:10.1016/j.jcis.2006.03.051.

[38] H. Lehle, E. Noruzifar, M. Oettel, Ellipsoidal particles at fluid interfaces, Eur. Phys. J. E. 26 (2008) 151–160. doi:10.1140/epje/i2007-10314-1.

[39] S. Ramos, A. Tanguy, Pinning-depinning of the contact line on nanorough surfaces., Eur. Phys. J. E. Soft Matter. 19 (2006) 433–40. doi:10.1140/epje/i2005-10056-0.

[40] S. Razavi, I. Kretzschmar, J. Koplik, C.E. Colosqui, S. Razavi, I. Kretzschmar, J. Koplik, C.E. Colosqui, Nanoparticles at liquid interfaces : Rotational dynamics and angular locking, J. Chem. Phys. (2014) 014904. doi:10.1063/1.4849135.

[41] A. Maestro, L.J. Bonales, H. Ritacco, T.M. Fischer, R.G. Rubio, F. Ortega, Surface rheology: macro- and microrheology of poly(tert-butyl acrylate) monolayers, Soft Matter. 7 (2011) 7761. doi:10.1039/c1sm05225j.